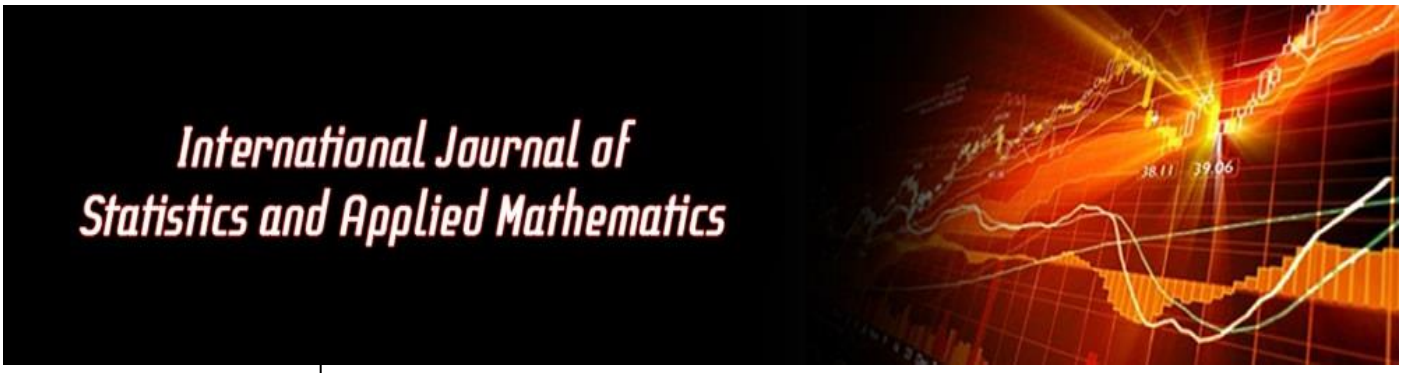


**ISSN:** 2456-1452
Maths 2020; 5(4): 01-11

www.mathsjournal.com
Received: 01-05-2020
Accepted: 03-06-2020

**AK Shukla**
Department of Mathematics,
Raja Shrikrishn Datt PG College
Jaunpur, Uttar Pradesh, India

**Shubham Kumar Dube**
Department of Mathematics,
Raja Shrikrishn Datt PG College
Jaunpur, Uttar Pradesh, India

**Corresponding Author:**
**AK Shukla**
Department of Mathematics,
Raja Shrikrishn Datt PG College
Jaunpur, Uttar Pradesh, India

# Numerical investigation for viscoelastic fluid flow past a vertical porous plate with variable suction under the impact of Soret Dufour effects, second-order chemical reaction and radiation

**AK Shukla and Shubham Kumar Dube**

**Abstract**
The object of this article is to monitor the change of second order chemical reaction and variable suction in MHD (magnetohydrodynamics) flow of viscoelastic fluid over a vertical porous plate immersed in a porous medium with radiation and Soret Dufour effects. The momentum, heat transfer, and mass transfer are set of nonlinear sets of partial differential equations impressed by boundary conditions, these equations are solved using finite difference method namely Crank-Nicolson. Obtained results of these physical variables are discussed by plotting graphs and numerical values of skin friction, Nusselt number and Sherwood number are studied by displaying the table.

**Keywords:** Viscoelastic fluid, MHD flow, Soret and Dufour effect, heat transfer, mass transfer, radiation, order of chemical reaction, finite difference method

## 1. Introduction
The fluid which follows the Newton law of viscosity like water, turpentine, solvents are viscous fluid and which does not follow Newton law i.e non-Newtonian like honey, toothpaste, polymer, paints, DNA suspension, some biological fluids are viscoelastic fluid. Nowadays, most of the research workers in this field are attracting research on viscoelastic fluids due to rheological applications in engineering and manufacturing processes.
Alsaedi *et al.* [1] examined MHD viscoelastic fluid flow with binary chemical reaction and Arrhenius activation energy using a numerical method. Gizachew and Shankar [2] discussed MHD flow and energy transfer in viscoelastic fluid expanded on a horizontal plate is considered. Alsulami *et al.* [3] inquired entropy generation in stratified Walters' B nanofluid with swimming gyrotactic microorganisms. Idowu and Falodun [4] investigated Soret–Dufour effects on MHD energy and species transfer of Walter's-B viscoelastic fluid over an infinite vertical plate. Malik and Rehman [5] explored the characteristics of second-order chemical reaction on steady MHD flow of viscous incompressible electrically conducting fluid in a porous media with heat and mass transfer. Singh *et al.* [6] given a survey for mixed convection hydromagnetic flow of an incompressible, electrically, and thermally conducting and chemically reacting viscoelastic fluid over a vertical porous channel immersed in a porous medium.
Megahed and Reddy [7] examined numerical and theoretical of the viscous dissipation phenomenon on the viscoelastic fluid flow which is passing over a stretching sheet. Rajakumar *et al.* [8] analyzed the influence of Dufour and thermal radiation on unsteady MHD Walter's liquid model-B flow past an impulsively started infinite vertical plate embedded in a porous medium with chemical reaction, Hall and ion-slip current. Sandeep *et al.* [9] examined the effects of radiation and variable heat source/sink on the boundary-layer flow of MHD fluid across a curved surface. Ramadevi *et al.* [10] delivered a numerical examination of 2D magnetohydrodynamic nonlinear micropolar fluid flow with radiation and stretching surface.
Induced by the above literature, this paper is focused on Soret-Dufour effects and second order chemical reaction on MHD flow of Walter's B viscoelastic fluid past over a porous plate with variable suction velocity and radiation.

The flow governing nonlinear partial differential equations is restored into a dimensionless system of PDEs with the help of appropriate boundary conditions and then solved by using Crank-Nicolson implicit finite difference method. The graphs have pictured the fields of velocity, temperature, and concentration profiles to the flow of relevant physical and chemical parameters. Further friction factor and coefficient of heat and mass transfer rates are tabled for these physical and chemical parameters.

## 2. Mathematical Model

Consider an unsteady magnetohydrodynamics flow of Walter's B viscoelastic fluid past over a porous plate imbedded in porous medium with variable heat and mass transfer under influence of Soret-Dufour effects, radiation effect and second-order chemical reaction. We considered a time dependent suction velocity normal to plate. $\bar{x}$-axis is considered along the plate and $\bar{y}$-axis is normal to it. Further, due to the semi-infinite plate, the flow variables are functions of normal distance $\bar{y}$ and $\bar{t}$ only. A uniform strength magnetic field $B_0$ is applied in direction of normal to the plate and the magnetic Reynolds number is assumed to be small so that stimulated magnetic field is negligible. The temperature and concentration of the plate surface are $T_p$ and $C_p$ respectively. Also, the free stream temperature and concentration are denoted by $T_\infty$ and $C_\infty$ respectively. With the above model, the governing equations of the flow under usual Boussinesq approximation are as follows:

$$\frac{\partial \bar{v}}{\partial \bar{y}} = 0 \tag{1}$$

$$\frac{\partial \bar{u}}{\partial \bar{y}} + \bar{v}\frac{\partial \bar{u}}{\partial \bar{t}} = \nu\frac{\partial^2 \bar{u}}{\partial \bar{y}^2} - \bar{\Gamma}\frac{\partial^3 \bar{u}}{\partial \bar{y}^2 \partial \bar{t}} + g\beta_t(T - T_\infty) + g\beta_c(C - C_\infty) - \frac{\sigma B_0^2 \bar{u}}{\rho} - \frac{\nu \bar{u}}{K_{per}} \tag{2}$$

$$\rho c_p\left(\frac{\partial T}{\partial \bar{y}} + \bar{v}\frac{\partial T}{\partial \bar{t}}\right) = k\frac{\partial^2 T}{\partial \bar{y}^2} - \frac{\partial R_d}{\partial \bar{y}} + \frac{\rho D_m K_T}{c_s}\frac{\partial^2 C}{\partial \bar{y}^2} \tag{3}$$

$$\frac{\partial C}{\partial \bar{y}} + \bar{v}\frac{\partial C}{\partial \bar{t}} = D_m\frac{\partial^2 C}{\partial \bar{y}^2} + \frac{D_m K_T}{T_m}\frac{\partial^2 T}{\partial \bar{y}^2} - K_r(C - C_\infty)^2 \tag{4}$$

together with boundary conditions for this model are as follows

$$\begin{gathered} \bar{t} \le 0\ \bar{u} = 0, T = T_\infty, C = C_\infty\ \forall\ \bar{y} \\ \bar{t} > 0\ \bar{u} = U_0, T = T_\infty + \epsilon\left(T_p - T_\infty\right)e^{-n\bar{t}}, C = C_\infty + \epsilon\left(C_p - C_\infty\right)e^{-n\bar{t}}, at\ \bar{y} = 0 \\ \bar{u} = 0\ T \to \infty\ C \to \infty, \bar{y} \to \infty. \end{gathered} \tag{5}$$

Integrating equation of continuity [1], we have constant or time dependent suction velocity. Since we have considered in this model already that there exists a variable suction velocity so we have time dependent suction velocity as

$$\bar{v} = -U_0\left(1 + \epsilon B e^{n\bar{t}}\right) \tag{6}$$

here $B$ denotes the suction parameter and $\epsilon B \ll 1$. Here $U_0$ is average constant suction velocity and the minus sign indicated that suction is outside the plate.

Using the Roseland approximation [11], we have the radiative heat flux $R_d$ as

$$R_d = -\frac{4\bar{\sigma}\partial T^4}{3a_r\partial \bar{y}} \tag{7}$$

We have considered that the temperature difference in the flow is very very small and $T^4$ can be written in a linear function of the temperature $T$. It is seen by expanding $T^4$ using a Taylor series about $T_\infty$, as follows

$$T^4 = T_\infty^4 + (T - T_\infty)3T_\infty^3 + \frac{(T - T_\infty)^2}{2!}12T_\infty^2 + \cdots \tag{8}$$

Neglecting higher order terms of $T_\infty$ in expansion, we have

$$T^4 \cong 4T_\infty^3 T - 3T_\infty^4. \tag{9}$$

Equation (3) is written in new form using equation (7) and (9)

$$\rho c_p\left(\frac{\partial T}{\partial \bar{y}} + \bar{v}\frac{\partial T}{\partial \bar{t}}\right) = k\frac{\partial^2 T}{\partial \bar{y}^2} + \frac{16\bar{\sigma}T_\infty^3}{3a_r}\frac{\partial^2 T}{\partial \bar{y}^2} + \frac{\rho D_m K_T}{c_s}\frac{\partial^2 C}{\partial \bar{y}^2}. \tag{10}$$

Introduction following non dimensional quantities

$$Df = \frac{D_m k_T (C_p - C_\infty)}{c_p c_s (T_p - T_\infty)}, So = \frac{D_m k_T (T_p - T_\infty)}{T_m \nu (C_p - C_\infty)}, \Omega = \frac{\bar{\Gamma} U_0^2}{\nu^2}, K = \frac{U_0^2 K_{per}}{\nu^2}, N = \frac{\nu n}{U_0^2}, y = \frac{\bar{y} U_0}{\nu}$$
$$Gr = \frac{\nu g \beta_t (T_p - T_\infty)}{U_0^3}, Gm = \frac{\nu g \beta_c (C_p - C_\infty)}{U_0^3}, \theta = \frac{(T - T_\infty)}{(T_p - T_\infty)}, \Phi = \frac{(C - C_\infty)}{(C_p - C_\infty)}, Pr = \frac{\mu c_p}{k} \quad (11)$$
$$R = \frac{4\bar{\sigma} T_\infty^3}{a_r k}, Ch = \frac{K_r \nu}{U_0^2}, Sc = \frac{\nu}{D_m}, u = \frac{\bar{u}}{U_0}, t = \frac{\bar{t} U_0^2}{\nu}, M = \frac{\sigma B_0^2 \nu}{\rho U_0^2}.$$

Using non dimensional quantities defined in equation (11) in equations (2), (4), (10), and (5) we have dimensionless form of governing equations and boundary conditions of flow as follows

$$\frac{\partial u}{\partial t} - (1 + \epsilon B e^{Nt}) \frac{\partial u}{\partial y} = \frac{\partial^2 u}{\partial y^2} - \Omega \frac{\partial^3 u}{\partial y^2 \partial t} + Gr\, \theta + Gm\, \Phi - \left(M + \frac{1}{K}\right) u \quad (12)$$
$$\frac{\partial \theta}{\partial t} - (1 + \epsilon B e^{Nt}) \frac{\partial \theta}{\partial y} = \frac{1}{Pr} \frac{\partial^2 \theta}{\partial y^2} + \frac{4R}{3} \frac{\partial^2 \theta}{\partial y^2} + Df \frac{\partial^2 \Phi}{\partial y^2} \quad (13)$$
$$\frac{\partial \Phi}{\partial t} - (1 + \epsilon B e^{Nt}) \frac{\partial \Phi}{\partial y} = \frac{1}{Sc} \frac{\partial^2 \Phi}{\partial y^2} + Sr \frac{\partial^2 \theta}{\partial y^2} - Ch \Phi^2 \quad (14)$$
$$t \le 0, u = 0, \theta = 0, \Phi = 0\ \forall y$$
$$t > 0, u = 1, \theta = 1 + \epsilon e^{-Nt}, \Phi = 1 + \epsilon e^{-Nt}, y = 0 \quad (15)$$
$$u = 0, \theta \to 0, \Phi \to 0, y \to \infty$$

The skin friction coefficient because of viscous drag in the vicinage of the walls is written in non dimensional form as

$$C_f = \left(-\frac{\partial u}{\partial y}\right)_{y=0} \quad (16)$$

Non dimensional form of Nusselt number because of the energy transfer between the fluid and wall is given as

$$N_\theta = \left(-\frac{\partial \theta}{\partial y}\right)_{y=0} \quad (17)$$

Non dimensional form of Sherwood number because of the mass transfer between the fluid and wall is given as

$$S_\Phi = \left(-\frac{\partial \Phi}{\partial y}\right)_{y=0} \quad (18)$$

## 3. Mathematical Solution

In this part of article, the Crank-Nicolson implicit finite difference method is applied on non dimensional governing partial differential equations (12)-(14) subject to conditions in equation (15) and we get transformed equations as follows

$$\frac{u_{l,m+1} - u_{l,m}}{\Delta t} - (1 - \epsilon B e^{Nj\Delta t}) \frac{u_{l+1,m} - u_{l,m}}{\Delta y} = \left(\frac{u_{l-1,m} - 2u_{l,m} + u_{l+1,m} - 2u_{l,m+1} + u_{l+1,m+1}}{2(\Delta y)^2}\right)$$
$$-\Omega \left(\frac{u_{l-1,m} - 2u_{l,m} + u_{l+1,m} - 2u_{l,m+1} + u_{l+1,m+1}}{2(\Delta y)^2 \Delta t}\right)$$
$$+Gr \left(\frac{\theta_{l,m+1} - \theta_{l,m}}{2}\right) + Gm \left(\frac{\Phi_{l,m+1} - \Phi_{l,m}}{2}\right) \quad (19)$$
$$-\left(M + \frac{1}{K}\right) \left(\frac{u_{l,m+1} + u_{l,m}}{2}\right)$$

$$\frac{\theta_{l,m+1} - \theta_{l,m}}{\Delta t} - (1 - \epsilon B e^{Nj\Delta t}) \frac{\theta_{l+1,m} - \theta_{l,m}}{\Delta y} = \frac{1}{Pr}\left(1 + \frac{4R}{3}\right) \left(\frac{\theta_{l-1,m} - 2\theta_{l,m} + \theta_{l+1,m} - 2\theta_{l,m+1} + \theta_{l+1,m+1}}{2(\Delta y)^2}\right)$$
$$+Df \left(\frac{\Phi_{l-1,m} - 2\Phi_{l,m} + \Phi_{l+1,m} - 2\Phi_{l,m+1} + \Phi_{l+1,m+1}}{2(\Delta y)^2}\right) \quad (20)$$

$$\frac{\theta_{l,m+1} - \theta_{l,m}}{\Delta t} - (1 - \epsilon B e^{Nj\Delta t}) \frac{\theta_{l+1,m} - \theta_{l,m}}{\Delta y} = \frac{1}{Sc} \left(\frac{\Phi_{l-1,m} - 2\Phi_{l,m} + \Phi_{l+1,m} - 2\Phi_{l,m+1} + \Phi_{l+1,m+1}}{2(\Delta y)^2}\right)$$
$$+So \left(\frac{\theta_{l-1,m} - 2\theta_{l,m} + \theta_{l+1,m} - 2\theta_{l,m+1} + \theta_{l+1,m+1}}{2(\Delta y)^2}\right) \quad (21)$$
$$-Ch \left(\frac{\Phi_{l,m+1} + \Phi_{l,m}}{2}\right)^2$$

with subject to conditions as given in transformed form

$$u_{l,0} = 0, \theta_{l,0} = 0, \Phi_{l,0} = 0, \forall l$$
$$u_{0,m} = 1, \theta_{0,m} = 1 + \epsilon e^{-Nm\Delta t}, \Phi_{0,m} = 1 + \epsilon e^{-Nm\Delta t} \quad (22)$$
$$u_{X,m} = 0, \theta_{X,m} \to 0, \Phi_{X,m} \to 0.$$

We divide $y$-axis using mess $y_l$, and $\Delta y = y_{l+1} - y_l$ and $t_m$ denotes partition of time $t$, $\Delta t = t_{m+1} - t_m$. Our aim is to calculate values of $u$, $\theta$ and $\Phi$ for different position of time $t$ i.e. $t + \Delta t$. For this first we substitute $l = 1,2,3,\cdots, X - 1$ where $X$ represents to $\infty$ because of in comparison to origin position $X$ is very very large. Thereby equations (19)-(21) generate tridiagonal system of non linear equations with subject to condition given in equation (22), are computed with the help of Thomas algorithm as

described in Wilkes *et al*. [XII], and fist we got the values of $\theta$ and $\Phi$ for all $y$ at time $t + \Delta t$ after this we replace values all values of $\theta$ and $\Phi$ for corresponding time $t + \Delta t$ then we get the values of velocity $u$ till desired time $t + \Delta t$.

## 4. Results and Discussion

In order to the discussion and demonstration, we obtained numerical results of governing non linear partial differential equations using Crank-Nicolson implicit finite difference method. The physical nature of the viscoelastic fluid flow are governed by the changing values of thermal Grashof number $Gr$, Solutal grashof number $Gm$, magnetic parameter $M$, Dufour number $Df$, Soret number $So$, chemical reaction parameter $Ch$, Schmidt number $Sc$, prandtl number $Pr$, permeability of porous medium $K$, viscoelastic parameter Ϙ, radiation parameter $R$, small reference parameter $\epsilon$, suction parameter $B$, constant $N$, and time $t$. The results for the changing of these physical parameters are given as functions of the non dimensional velocity $u$, the non dimensional temperature $\theta$ and non dimensional concentration $\Phi$.

Fig. 1 and Fig. 2 depict that an increase in Dufour number results an increase in velocity profiles and an increase in temperature profiles respectively. While in Fig. 3 near to plate concentration decreases after that mid of boundary layer of concentration it increase slowly as Dufour number increases. Fig. 4, Fig. 5 and Fig. 6 show the change of chemical reaction parameter $Ch$ in velocity, temperature and concentration profiles respectively. It is analyzed that velocity profiles decrease and temperature profiles increase near to plate whereas concentration profiles increases very fast in compare to velocity or temperature profiles. The effect of Soret number on velocity, temperature and concentration profiles display in Fig. 7, Fig. 8 and Fig. 9 respectively. It is analyzed when soret number increases velocity profiles increases rapidly in Fig. 7. In Fig. 8, Temperature profiles near to plate decrease, and after mid of thermal boundary layer it increases when soret number increases. Fig. 9 demonstrates that concentration profiles increases very fast as soret number changes. Fig. 10 shows the effects of change in magnetic parameter $M$ that velocity profiles increases rapidly as $M$ increases. Velocity profiles decreases in Fig. 11, temperature profiles decreases very fast in Fig. 12 when prandtl number $Pr$ increases.

In Fig. 13, concentration profiles first near to plate increases after that decreases as $Pr$ increases. It is noticed that boundary layer of momentum, thermal and species all increase as radiation increase in Fig. 14-16. Fig. 14 depicts that velocity profiles show increment at extreme of boundary layer when radiation parameter $R$ increases. Fig. 15 shows effect of change of radiation parameter $R$ that temperature profiles increases rapidly as $R$ increases. Concentration profiles in Fig. 16 first near to plate decreases after mid of boundary layer it increase as $R$ increases. The effects of Schmidt number $Sc$ in velocity profiles, temperature profiles and concentration profiles are analyzed in Fig. 17-19. It shows that velocity profiles decreases and concentration profiles increases very fast when $Sc$ increases while temperature profiles first increases after then decreases as increases $Sc$. It is very interesting change in velocity profiles when viscoelastic parameter changes in Fig. 20. It is seen that just near to plate it increases after then it decreases. Rapid changes has been noticed in Fig. 21-23 that velocity profiles, temperature profiles and concentration profiles increase when time $t$ increases. Table 1 represents the influence of Dufour number $Df$, Soret number $So$, Magnetic parameter $M$, chemical reaction parameter $Ch$, Prandtl number $Pr$, Schmidt number $Sc$, radiation parameter $R$, viscoelastic parameter Ϙ, and time $t$ on skin friction coefficient $C_f$, Nusselt number $N_\theta$, and Sherwood number $S_\Phi$. It is analyzed that skin friction coefficient increases when Dufour number, Soret number, Schmidt number, radiation parameter, viscoelastic parameter, and time increase whereas it decreases as chemical reaction parameter, magnetic parameter, and prandtl number increase. Table 1 shows that Nusselt number $N_\theta$ decreases as Dufour number, chemical reaction parameter, Schmidt number, radiation parameter, and time increase while $N_\theta$ increases when prandtl number and soret number increase. Table 1 illustrates that increase of Dufour number, chemical reaction parameter, Schmidt number, and radiation parameter result as Sherwood number $S_\Phi$ increases while $S_\Phi$ increases on increment of prandtl number, soret number, and time.

## 5. Conclusion

The investigation of Soret-Dufour, radiation, and second order chemical reaction effects on an unsteady MHD viscoelastic fluid flow past over a infinite vertical porous plate immersed in porous medium in presence of variable temperature, concentration, and variable suction velocity. The impact of some valuable flow governing physical parameters on these flow variables have been utterly dissertated in the previous section. The pre-dominant results are as follows

1. The effect of chemical reaction on viscoelastic fluid is to decrease boundary layer thickness of momentum and increases boundary layer thickness of species.
2. There is interesting change has been seen for viscoelastic parameter in momentum of fluid i.e. fluid velocity near to plate first increase and after that it decreases,
3. Thermal and species boundary layer thickness increase at increase of Dufour number.
4. Speices and thermal boundary layer thickness increase at increase of Soret number.

## 6. Acknowledgement

I would like to express my special thanks of gratitude to my principal Dr. Vishnu Chandra Tripathi, vice-principal Dr. Mayanand Upadhyay, and our proctor of science faculty Dr. A.K. Dwivedi who encourage us to complete this research work.

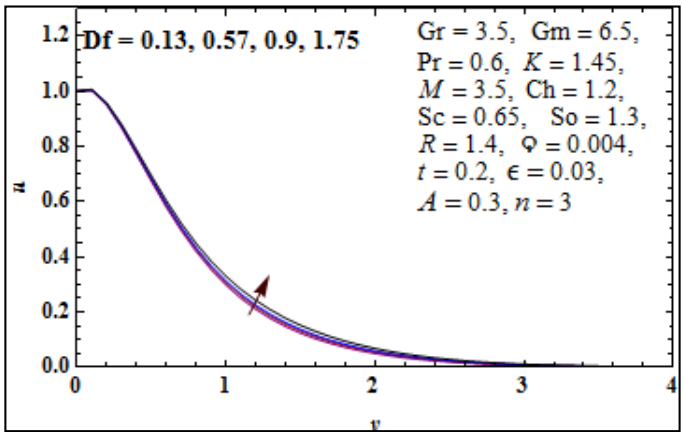


**Fig 1:** Velocity profiles Vs Dufour number

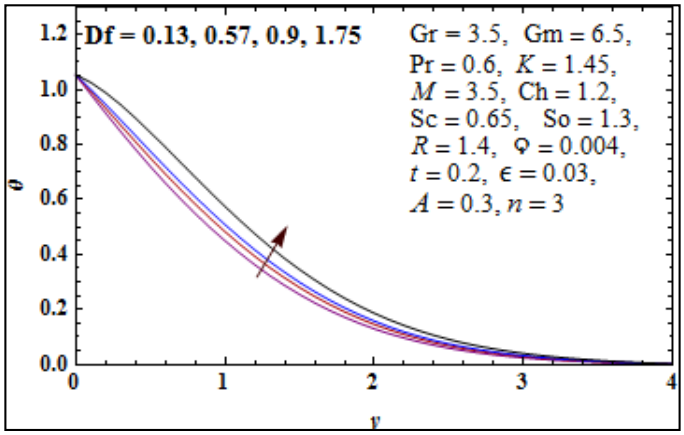


**Fig 2:** Temperature profiles Vs Dufour number

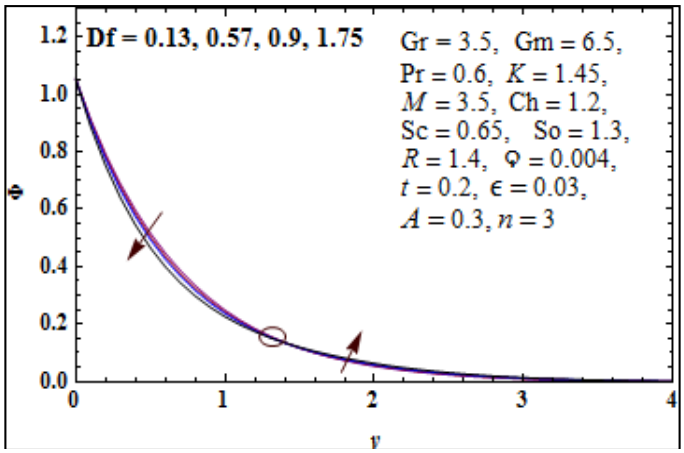


**Fig 3:** Concentration profiles Vs Dufour number

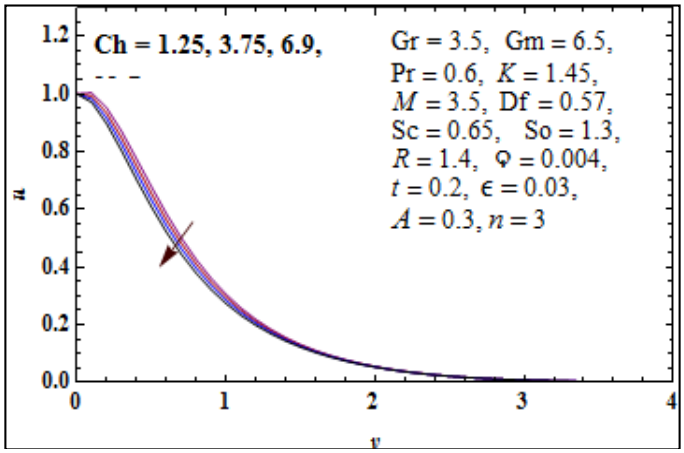


**Fig 4**: Velocity profiles Vs $Ch$

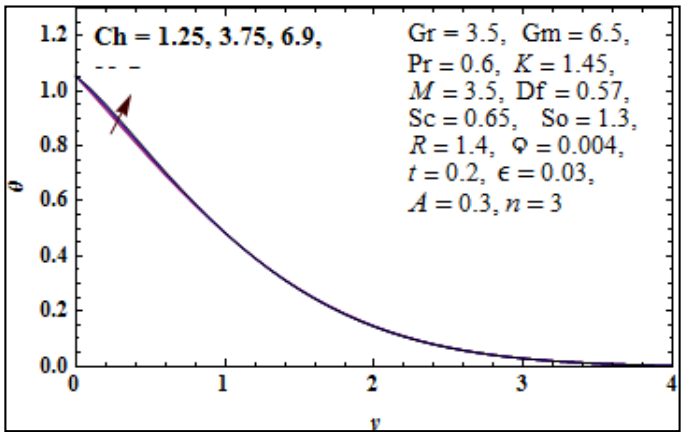


**Fig 5:** Temperature profiles Vs $Ch$

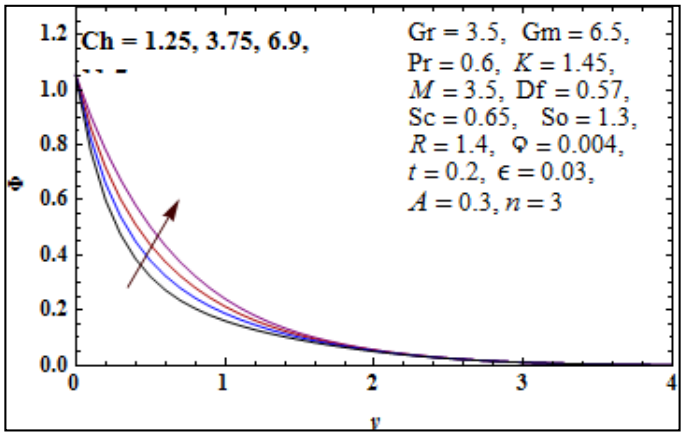


**Fig 6:** Concentration profiles Vs $\boldsymbol{Ch}$

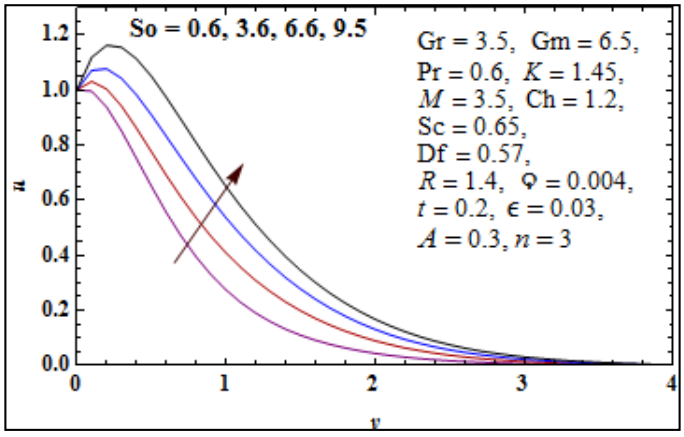


**Fig 7:** Velocity profiles Vs Soret number

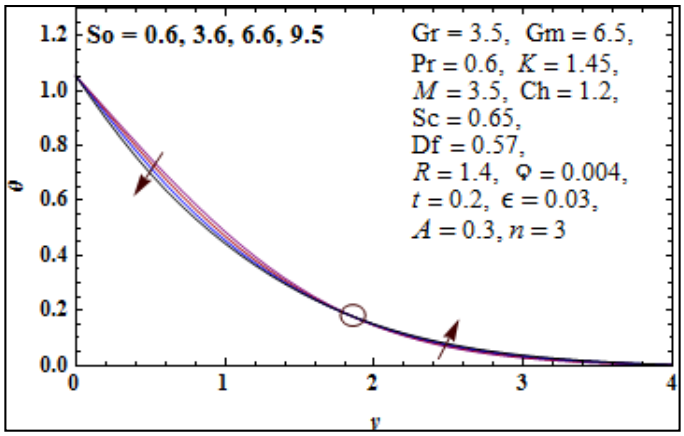


**Fig 8:** Temperature profiles Vs Soret number

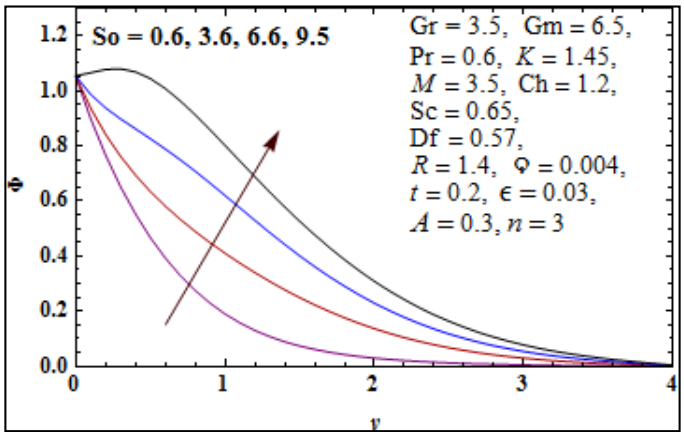


**Fig 9:** Concentration profiles Vs Soret number

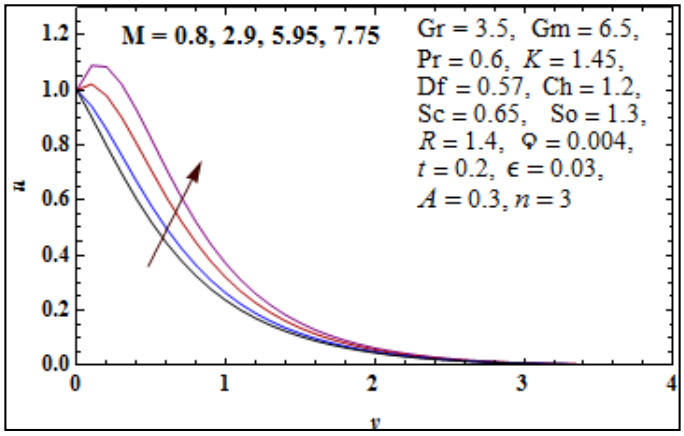


**Fig 10:** Velocity profiles Vs magnetic parameter

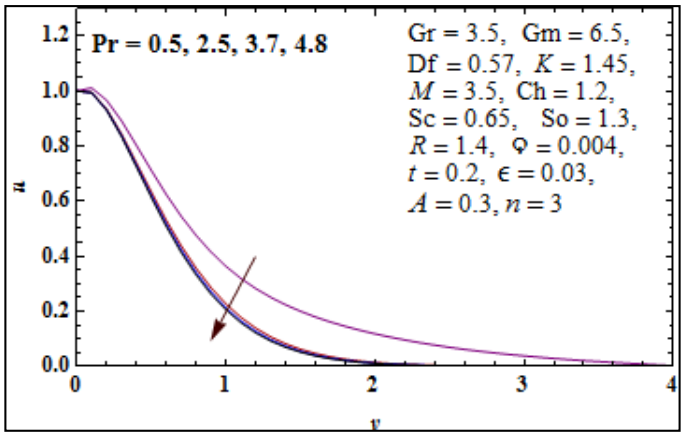


**Fig 11:** Velocity profiles Vs Prandtl number

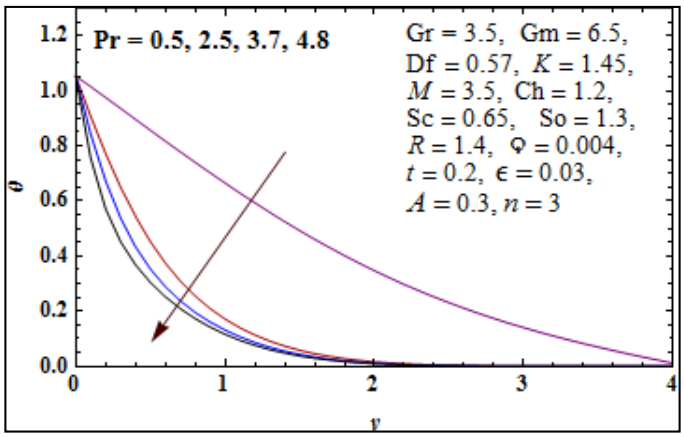


**Fig 12:** Temperature profiles Vs Prandtl number

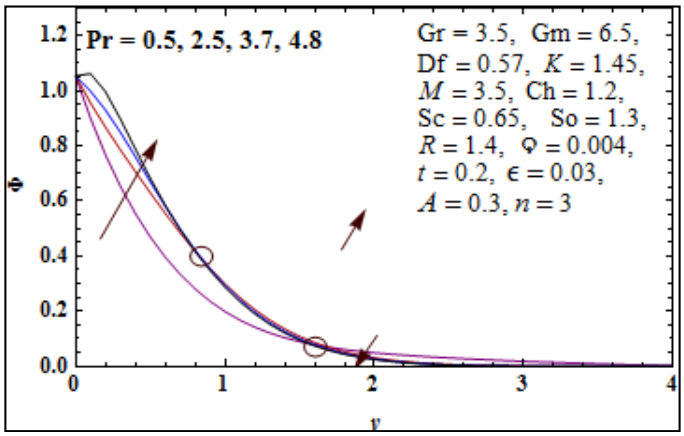


**Fig 13:** Concentration profiles Vs Prandtl number

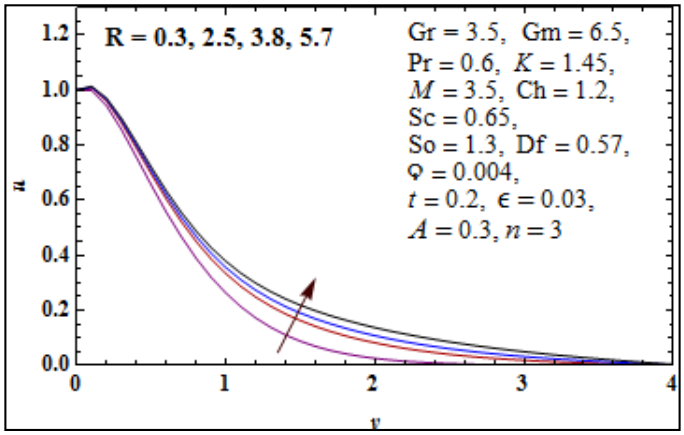


**Fig 14:** Velocity profiles Vs radiation

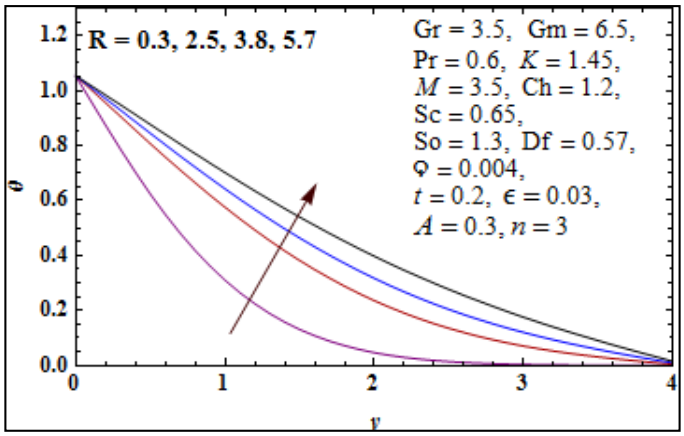


**Fig 15:** Temperature profiles Vs radiation

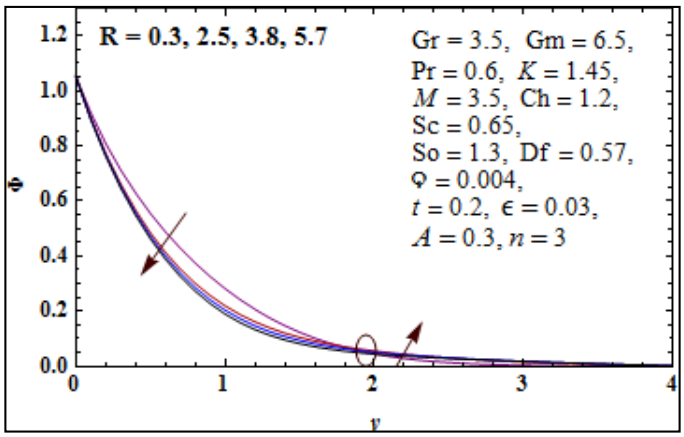


**Fig 16:** Concentration profiles Vs radiation

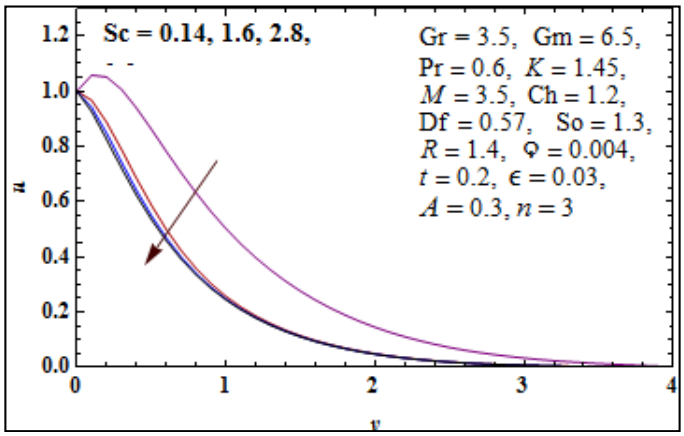


**Fig 17:** Velocity profiles Vs Schmidt number

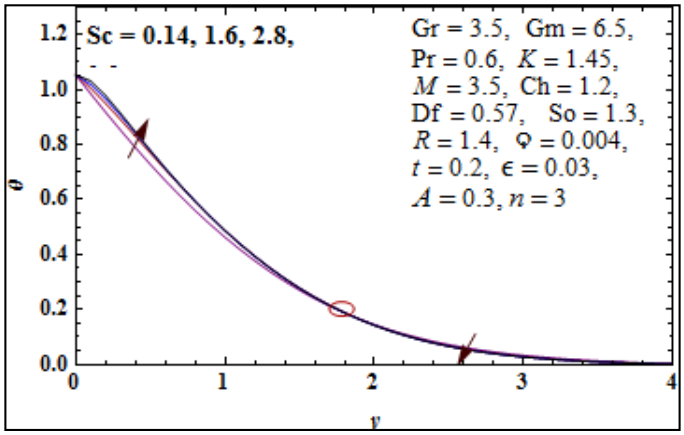


**Fig 18:** Temperature profiles Vs Schmidt number

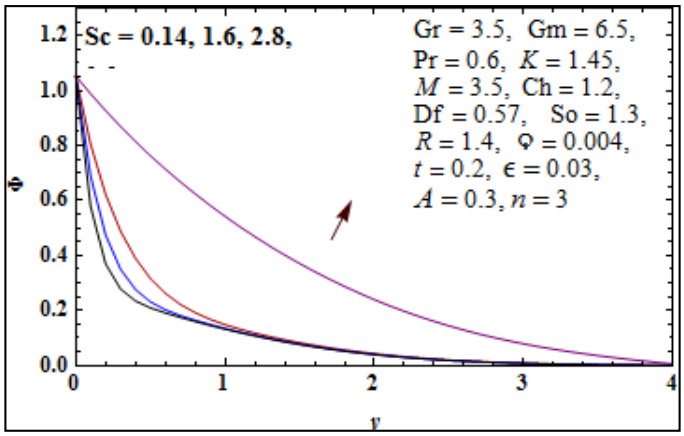


**Fig 19:** Concentration profiles Vs Schmidt number

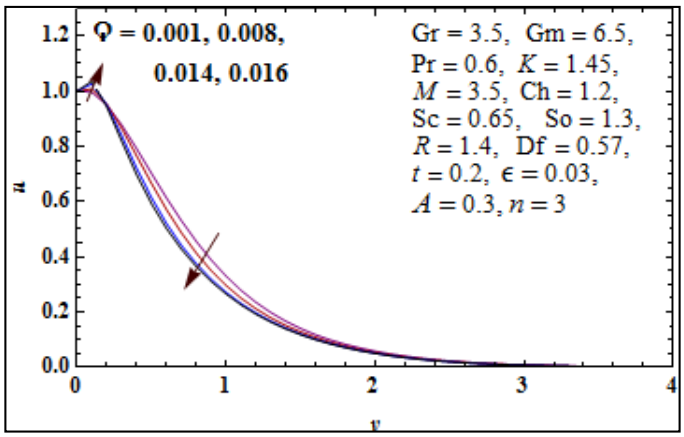


**Fig 20:** Velocity profiles Vs viscoelastic parameter

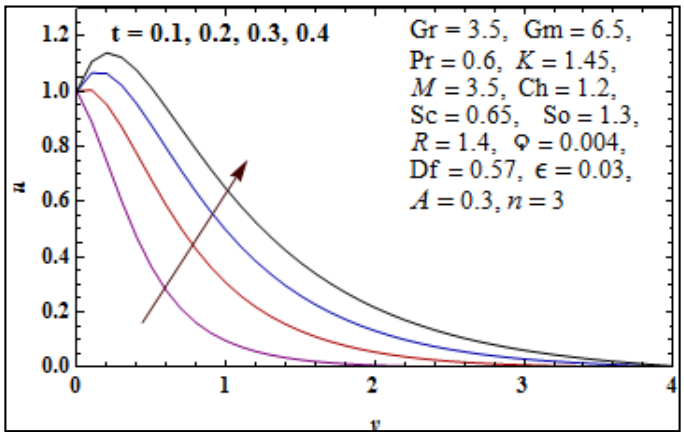


**Fig 21:** Velocity profiles Vs time

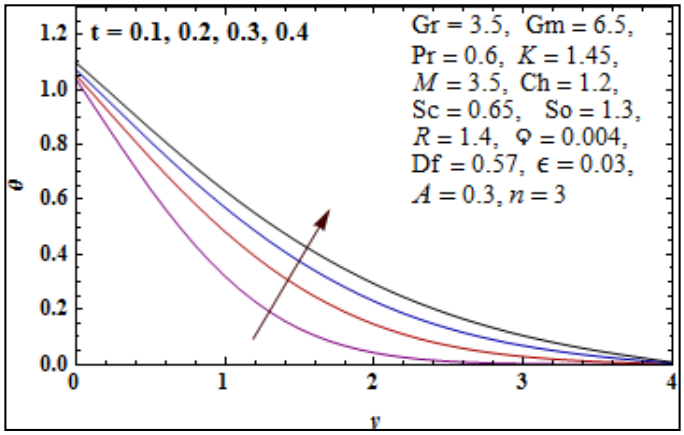


**Fig 22:** Temperature profiles Vs time

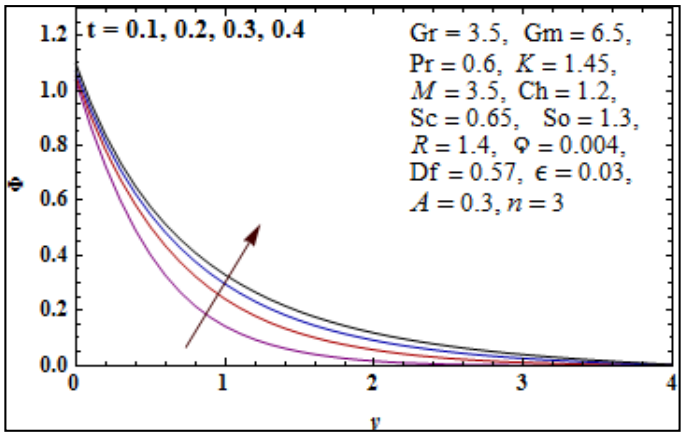


**Fig 23:** Concentration profiles Vs time

**Table 1**: Skin Friction, Nusselt number, Sherwood number for various physical parameter

| $Df$ | $M$ | $So$ | $Ch$ | $Sc$ | $R$ | $Pr$ | Γ | $t$ | $C_f$ | $N_\theta$ | $S_\Phi$ |
|---|---|---|---|---|---|---|---|---|---|---|---|
| 0.13 | 3.5 | 1.3 | 1.2 | 0.65 | 1.4 | 0.6 | 0.004 | 0.2 | 0.0251591 | 0.704167 | 1.40807 |
| 0.9 | 3.5 | 1.3 | 1.2 | 0.65 | 1.4 | 0.6 | 0.004 | 0.2 | 0.0431731 | 0.524467 | 1.50942 |
| 1.75 | 3.5 | 1.3 | 1.2 | 0.65 | 1.4 | 0.6 | 0.004 | 0.2 | 0.0629846 | 0.278915 | 1.65414 |
| 0.57 | 0.8 | 1.3 | 1.2 | 0.65 | 1.4 | 0.6 | 0.004 | 0.2 | 0.885269 | 0.605557 | 1.46318 |
| 0.57 | 2.9 | 1.3 | 1.2 | 0.65 | 1.4 | 0.6 | 0.004 | 0.2 | 0.208842 | 0.605557 | 1.46318 |
| 0.57 | 5.95 | 1.3 | 1.2 | 0.65 | 1.4 | 0.6 | 0.004 | 0.2 | -0.596868 | 0.605557 | 1.46318 |
| 0.57 | 7.75 | 1.3 | 1.2 | 0.65 | 1.4 | 0.6 | 0.004 | 0.2 | -0.996156 | 0.605557 | 1.46318 |
| 0.57 | 3.5 | 0.6 | 1.2 | 0.65 | 1.4 | 0.6 | 0.004 | 0.2 | -0.0434961 | 0.597282 | 1.54551 |
| 0.57 | 3.5 | 3.6 | 1.2 | 0.65 | 1.4 | 0.6 | 0.004 | 0.2 | 0.308705 | 0.636399 | 1.16483 |
| 0.57 | 3.5 | 6.6 | 1.2 | 0.65 | 1.4 | 0.6 | 0.004 | 0.2 | 0.709897 | 0.690403 | 0.665942 |
| 0.57 | 3.5 | 9.5 | 1.2 | 0.65 | 1.4 | 0.6 | 0.004 | 0.2 | 1.18243 | 0.778584 | -0.113747 |
| 0.57 | 3.5 | 1.3 | 1.25 | 0.65 | 1.4 | 0.6 | 0.004 | 0.2 | 0.0329202 | 0.604477 | 1.4733 |
| 0.57 | 3.5 | 1.3 | 3.75 | 0.65 | 1.4 | 0.6 | 0.004 | 0.2 | -0.0760636 | 0.558194 | 1.9024 |
| 0.57 | 3.5 | 1.3 | 6.9 | 0.65 | 1.4 | 0.6 | 0.004 | 0.2 | -0.179185 | 0.514663 | 2.29933 |
| 0.57 | 3.5 | 1.3 | 11.7 | 0.65 | 1.4 | 0.6 | 0.004 | 0.2 | -0.293672 | 0.465937 | 2.73716 |

| | | | | | | | | | | | |
|---|---|---|---|---|---|---|---|---|---|---|---|
| 0.57 | 3.5 | 1.3 | 1.2 | 0.14 | 1.4 | 0.6 | 0.004 | 0.2 | 0.575717 | 0.689555 | 0.653769 |
| 0.57 | 3.5 | 1.3 | 1.2 | 1.6 | 1.4 | 0.6 | 0.004 | 0.2 | -0.339494 | 0.490294 | 2.4901 |
| 0.57 | 3.5 | 1.3 | 1.2 | 2.8 | 1.4 | 0.6 | 0.004 | 0.2 | -0.589314 | 0.356752 | 3.65299 |
| 0.57 | 3.5 | 1.3 | 1.2 | 3.9 | 1.4 | 0.6 | 0.004 | 0.2 | -0.745367 | 0.229049 | 4.75606 |
| 0.57 | 3.5 | 1.3 | 1.2 | 0.65 | 0.3 | 0.6 | 0.004 | 0.2 | -0.0188724 | 0.901869 | 1.32024 |
| 0.57 | 3.5 | 1.3 | 1.2 | 0.65 | 2.5 | 0.6 | 0.004 | 0.2 | 0.069791 | 0.489114 | 1.50992 |
| 0.57 | 3.5 | 1.3 | 1.2 | 0.65 | 3.8 | 0.6 | 0.004 | 0.2 | 0.0981585 | 0.413059 | 1.53693 |
| 0.57 | 3.5 | 1.3 | 1.2 | 0.65 | 5.7 | 0.6 | 0.004 | 0.2 | 0.127034 | 0.349191 | 1.55773 |
| 0.57 | 3.5 | 1.3 | 1.2 | 0.65 | 1.4 | 0.5 | 0.004 | 0.2 | 0.108688 | 0.388286 | 1.54515 |
| 0.57 | 3.5 | 1.3 | 1.2 | 0.65 | 1.4 | 2.5 | 0.004 | 0.2 | -0.0584405 | 1.45832 | 0.990039 |
| 0.57 | 3.5 | 1.3 | 1.2 | 0.65 | 1.4 | 3.7 | 0.004 | 0.2 | -0.0688028 | 2.09899 | 0.555433 |
| 0.57 | 3.5 | 1.3 | 1.2 | 0.65 | 1.4 | 4.8 | 0.004 | 0.2 | -0.0668827 | 2.97099 | -0.080427 |
| 0.57 | 3.5 | 1.3 | 1.2 | 0.65 | 1.4 | 0.6 | 0.001 | 0.2 | -0.0374745 | 0.605557 | 1.46318 |
| 0.57 | 3.5 | 1.3 | 1.2 | 0.65 | 1.4 | 0.6 | 0.008 | 0.2 | 0.0749238 | 0.605557 | 1.46318 |
| 0.57 | 3.5 | 1.3 | 1.2 | 0.65 | 1.4 | 0.6 | 0.014 | 0.2 | 0.258789 | 0.605557 | 1.46318 |
| 0.57 | 3.5 | 1.3 | 1.2 | 0.65 | 1.4 | 0.6 | 0.016 | 0.2 | 0.354827 | 0.605557 | 1.46318 |
| 0.57 | 3.5 | 1.3 | 1.2 | 0.65 | 1.4 | 0.6 | 0.004 | 0.1 | -1.12131 | 0.822383 | 1.69248 |
| 0.57 | 3.5 | 1.3 | 1.2 | 0.65 | 1.4 | 0.6 | 0.004 | 0.2 | 0.0354453 | 0.605557 | 1.46318 |
| 0.57 | 3.5 | 1.3 | 1.2 | 0.65 | 1.4 | 0.6 | 0.004 | 0.3 | 0.654522 | 0.517032 | 1.41156 |
| 0.57 | 3.5 | 1.3 | 1.2 | 0.65 | 1.4 | 0.6 | 0.004 | 0.4 | 1.06888 | 0.473874 | 1.42065 |

## 7. References


1. Alsaedi A, Hayat T, Mustafa M, Mushtaq A. Numerical Study of MHD Viscoelastic Fluid Flow with Binary Chemical Reaction and Arrhenius Activation Energy. Int. J Chem. React. Eng. 2016; 15(1):1-9.
2. Gizachew Adamu, Shankar Bandari. MHD Flow of Non-Newtonian Viscoelastic Fluid on Stretching Sheet with The Effect of Slip Velocity. International Journal of Engineering and Manufacturing Science. 2018; 8(1):1-14.
3. Alsulami Hamed, Tariq Sana, Naz Rahila. Inquiry of entropy generation in stratified Walters' B nanofluid with swimming gyrotactic microorganisms. Alexandria Engineering Journal. 2020; 59:247–261.
4. Idowu AS, Falodun BO. Soret–Dufour effects on MHD heat and mass transfer of Walter's-B viscoelastic fluid over a semi-infinite vertical plate: spectral relaxation analysis. Journal of Taibah University for Science. 2019; 13(1):49-62.
5. Malik MY, Rehman Khalil-ur. Effects of Second Order Chemical Reaction on MHD Free Convection Dissipative Fluid Flow past an Inclined Porous Surface by way of Heat Generation: A Lie Group Analysis. Inf. Sci. Lett. 2016; 5(2):35-45.
6. Singh JK, Seth GS, Joshi Naveen, Srinivasa CT. Mixed convection flow of a viscoelastic fluid through a vertical porous channel influenced by a moving magnetic field with Hall and ion-slip currents, rotation, heat radiation and chemical reaction. Bulgarian Chemical Communications. 2020; 52(1):147-158.
7. Ahmed M, Megahed M, Gnaneswara Reddy. Numerical treatment for MHD viscoelastic fluid flow with variable fluid properties and viscous dissipation. Indian J Phys. 2020; https://doi.org/10.1007/s12648-020-01717-3.
8. Rajakumar KVB, Govinda Rao T, Reddy Umasankara M, Balamurugan KS. Influence of Dufour and thermal radiation on unsteady MHD Walter's liquid model-B flow past an impulsively started infinite vertical plate embedded in a porous medium with chemical reaction, Hall and ion slip current. SN Appl. Sci. 2020; 2:742. https://doi.org/10.1007/s42452-020-2484-y.
9. Sandeep N, Reddy JVR, Anantha K Kumar, Sugunamma V. Simultaneous solutions for MHD flow of Williamson fluid over a curved sheet with non-uniform heat source/sink. Heat Transf Res. 2019; 50(6):581-603.
10. Ramadevi B, Anantha Kumar K, Sugunamma V, Ramana Reddy JV, Sandeep N. Magnetohydrodynamic mixed convective flow of micropolar fluid past a stretching surface using modified Fourier's heat flux model. Journal of Thermal Analysis and Calorimetry. 2019; https://doi.org/10.1007/s10973-019-08477-1.
11. Siegel R, Howell JR. Thermal Radiation Heat Transfer. Taylor & Francis, London, 1992.
12. Wilkes JO, Luther HA, Carnahan B. Applied Numerical Methods. Krieger Pub Co, Florida, 1990.